doi:10.1017/S1431927622006778
Microsc. Microanal. 28 (Suppl 1), 2022

Unravelling Temperature-Dependent Ordered Skyrmion Phases in Magnetic Layered Materials using Lorentz transmission Electron Microscopy

Reed Yalisove[1,2]*, Sandhya Susarla[2], Hongrui Zhang[1], Rui Chen[1,3], Xiang Chen[3,4], Robert J. Birgeneau[3,4], Jie Yao[1,3], Ramamoorthy Ramesh[1] and Mary Scott[1,2]

[1.] University of California, Berkeley, Department of Materials Science and Engineering, Berkeley, CA, United States.
[2.] Lawrence Berkeley National Lab, National Center for Electron Microscopy, Berkeley, CA, United States.
[3.] Lawrence Berkeley National Lab, Materials Sciences Division, Berkeley, CA, United States.
[4.] University of California, Department of Physics, Berkeley, CA, United States .
* Corresponding author: yalisove@berkeley.edu

Lorentz transmission electron microscopy (LTEM) is an exciting platform for the study of topological magnetic textures in materials, allowing imaging of magnetic domains and skyrmions under a variety of temperature and field conditions [1, 2]. Co-doped Fe_5GeTe_2 (FCGT) is a two-dimensional Van der Waals ferromagnet that exhibits room temperature, zero-field skyrmions when doped to precisely 50% Co concentration [3]. Recent studies have probed the temperature-magnetic field phase diagram of magnetic domain structures in this material with electrical transport measurements, but skyrmions tend to undergo complex 2D phase transitions that are best examined through real-space imaging techniques such as LTEM [4]. Fast, robust identification of skyrmions is required to study skyrmion ordering and dynamics of this type. Huang et al. have had success identifying Bloch-type skyrmions using Laplacian of Gaussian (LoG) filters on raw LTEM images, but skyrmion identification remains a challenging problem [4]. The Néel skyrmions in FCGT present further challenges due to their non-circular geometry, very low contrast, and proximity to regular magnetic domains and non-magnetic sample features, as in Figure 1a.

Here we present a new, topology-inspired method for identifying and locating Néel skyrmions. By anticipating a skyrmion's topological winding and analyzing the sample's magnetization vector map, we can reliably locate Néel skyrmions in FCGT. Néel skyrmions can be identified by a human viewer (sitting far from the page) in Figure 1a, and transport of intensity equation (TIE) reconstruction of the magnetization in the sample makes the skyrmions very apparent (Fig. 1b). This TIE reconstruction used the pyLorentz package [5]. The in-plane magnetization of a Néel skyrmion viewed with a slight α tilt, Figure 1c, is prescribed by theory. The x- and y- components of this field are convolved with simple square kernels with dimension shown in figure 1b as dashed boxes. This convolution creates patterns, shown in Figure 1d,e, for the x- and y- components, respectively, which may be easily located via an additional convolution. The resulting map of skyrmions is shown in Figure 1f. This method reliably locates skyrmions in an LTEM image, especially when the locations of domains in the sample are considered.

We construct a temperature-field phase diagram of FCGT using this identification method to quantify skyrmion ordering. Figure 2a-d shows the skyrmion patterns detected in several example images across a range of magnetic fields. Here, the sample was tilted to +18° in order to create contrast in the Néel-type domain walls, and magnetic field was increased by increasing the electrical current in the objective lens. A variety of arrangements are shown, including helical domains at low field (Fig. 2a), ordered skyrmions (Fig. 2b), disordered skyrmions (Fig. 2c), and the magnetically saturated sample at high field (Fig. 2d). Skyrmions are reliably located across a range of magnetic fields with minimal false positives at helical domains and structural defects. Distributions of inter-skyrmion distances were calculated from the arrangement of skyrmions in each image, which are presented across a range of temperatures and fields in Figure 2e-h. A peak in this distribution corresponds to local skyrmion ordering with a periodicity equal to the given radius; a noisy, flat signal suggests no ordering. This data is used to locate the regions of the temperature field phase diagram (Fig. 2i) that features skyrmion lattice.

Using topology as a tool for skyrmion identification will enable fast, reliable analysis of skyrmion ordering and dynamics for a range of in-situ LTEM experiments [6].

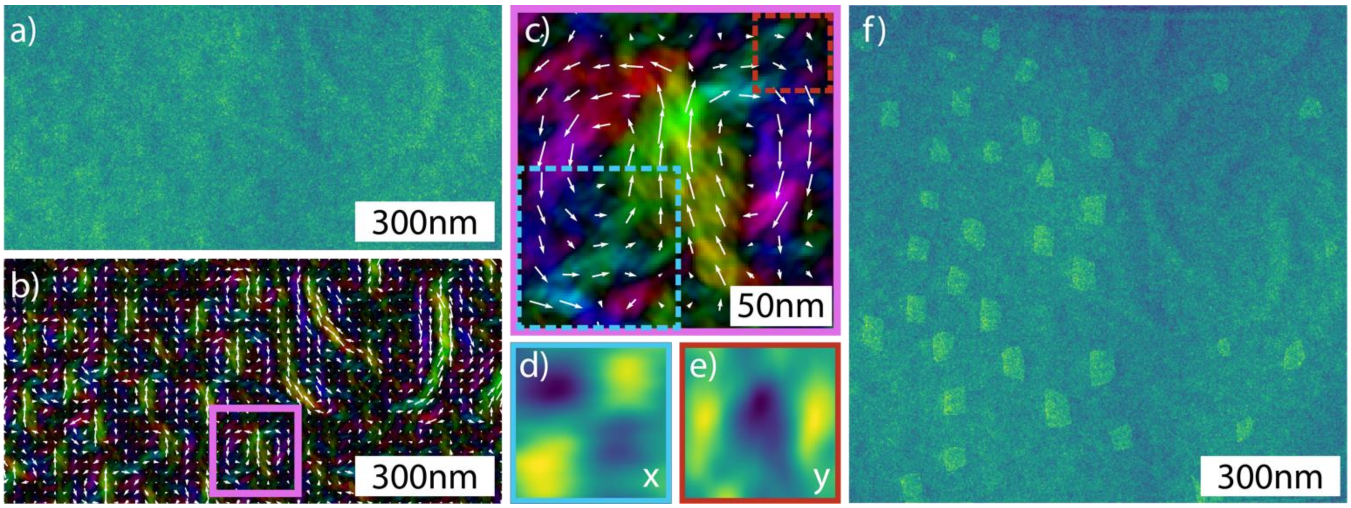

Figure 1. LTEM **(a)** and magnetization vector reconstruction **(b)** of the same region in an FCGT sample at 270K with 18°α-tilt showing both skyrmions (left) and helical domains (right) Skyrmions are most easily viewed from a distance. **b)** Detailed view of single skyrmion from (a). The x- (**c**) and y- (**d**) components of the magnetization vectors are convolved with squares (shown as dashed rectangles in (b) to yield characteristic patterns that can be used to identify skyrmions. **e)** Mask indicating skyrmion location overlaid on LTEM image from (a).

https://doi.org/10.1017/S1431927622006778 Published online by Cambridge University Press

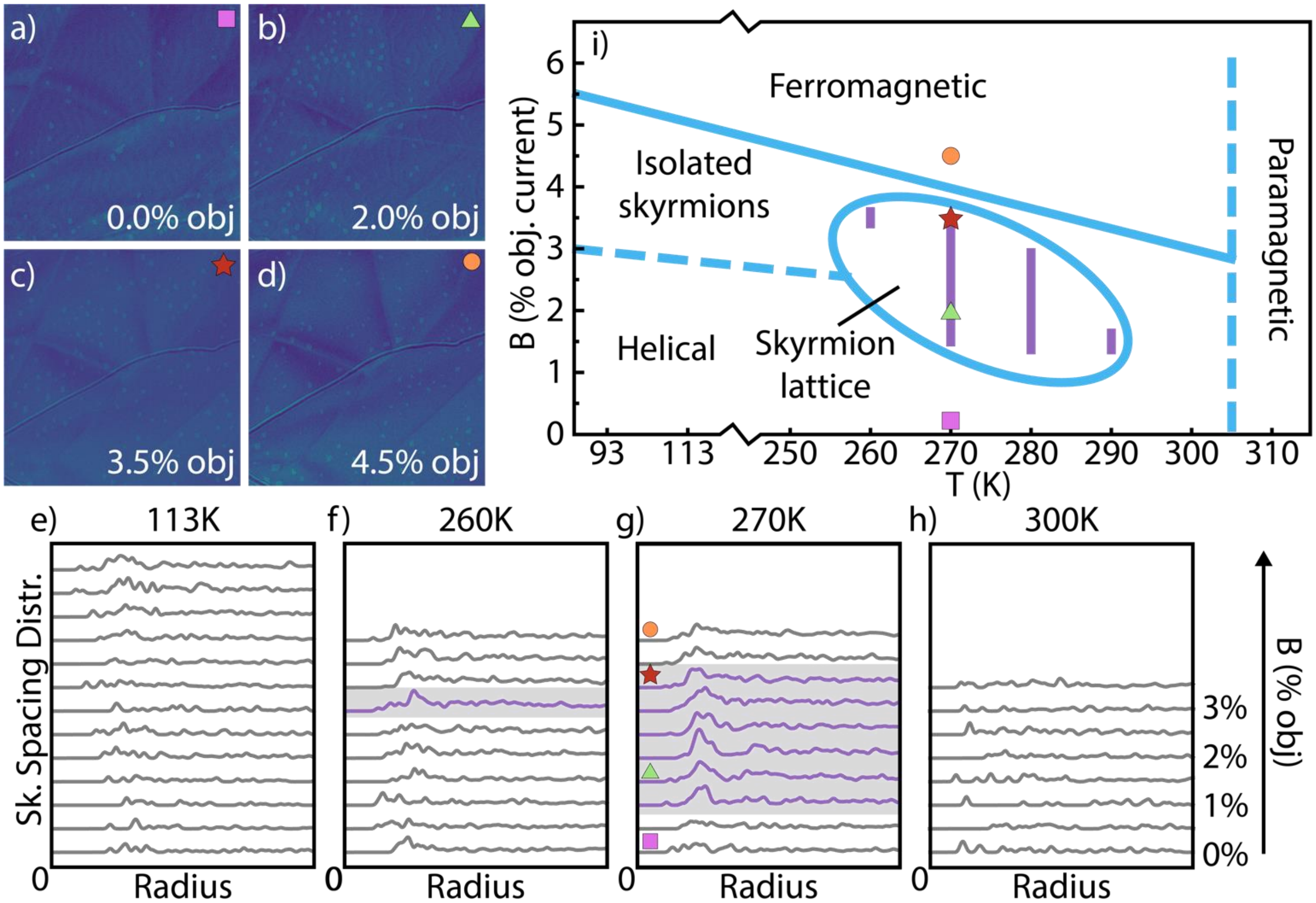

Figure 2. (a-d) LTEM images at 270K with skyrmion masks showing **a)** helical domains, **b)** skyrmion lattice, **c)** disordered skyrmions, **d)** saturated sample. **(e-h)** Inter-skyrmion spacing distribution of detected skyrmions in series of images with increasing magnetic field, at different temperatures. **i)** Temperature-magnetic field phase diagram created from skyrmion distribution data series. The marked isothermal lines correspond to distributions in (e-h) that display periodicity, highlighted in gray. Conditions for images in (a-d) are marked.

References:

[1] M. Hale, H. Fuller, H. Rubinstein, Journal of Applied Physics **30** (1959) p. 789. doi:10.1063/1.1735233
[2] X. Yu et al., Nature **465** (2010), p. 901. doi:10.1038/nature09124
[3] H. Zhang et al. Science Advances (2022), p. eabm7103. doi:10.48550/arXiv.2106.00833
[4] P. Huang et al. Nature Nanotechnology **15** (2020), p. 761. doi:10.1038/s41565-020-0716-3
[5] A. McCray et al. Physical Review Applied **15** (2021), p. 044025. doi:10.1103/PhysRevApplied.15.044025
[6] R. Y. is supported by the National Science Foundation Graduate Research Fellowship under Grant No. DGE 2146752. Work at the Molecular Foundry was supported by the Office of Science, Office of Basic Energy Sciences, of the U.S. Department of Energy under Contract No. DE-AC02-05CH11231.

https://doi.org/10.1017/S1431927622006778 Published online by Cambridge University Press